

Human-inspired Explanations for Vision Transformers and Convolutional Neural Networks

Mahadev Prasad Panda¹, Matteo Tiezzi², Martina Vilas³, Gemma Roig⁴, Bjoern M. Eskofier^{1,5}, and Dario Zanca^{1,*}

¹ Department AIBE, FAU Erlangen-Nürnberg, Erlangen, Germany

² PAVIS, Istituto Italiano di Tecnologia (IIT), 16163, Genova, Italy

³ Ernst Strüngmann Institute for Neuroscience, Frankfurt am Main, Germany

⁴ Goethe-Universität Frankfurt am Main, Frankfurt am Main, Germany

⁵ Institute of AI for Health, Helmholtz Zentrum München, Munich, Germany

* ✉ dario.zanca@fau.de

Abstract. We introduce Foveation-based Explanations (FovEx), a novel human-inspired visual explainability (XAI) method for Deep Neural Networks. Our method achieves state-of-the-art performance on both transformer (on 4 out of 5 metrics) and convolutional models (on 3 out of 5 metrics), demonstrating its versatility. Furthermore, we show the alignment between the explanation map produced by FovEx and human gaze patterns (+14% in NSS compared to RISE, +203% in NSS compared to gradCAM), enhancing our confidence in FovEx’s ability to close the interpretation gap between humans and machines.

Keywords: Foveation-based Explanation · Explainable AI

1 Introduction

Motivations & Related Work. While various explanation methods have been developed for deep learning vision models [2–4, 21], these approaches are often tailored to specific architectures and lack universality. Though gradCAM and its derivations [2, 21] are effective XAI methods for convolutional architectures, they are adversely affected by certain architectural attributes of vision transformers, such as skip connections, non-local self-attention mechanisms, and unstable gradients [5]. On the other side, XAI methods for vision transformers [1, 3, 4] are often tailored to transformer-specific characteristics, such as attention weights or class tokens, making their application to convolutional-based models unfeasible. Additionally, current XAI methods often lack contextual aspects that make such explanations understandable to humans [12, 16]. Incorporating insights from biological vision mechanisms into XAI frameworks can enhance the quality of explanations and make them more aligned to human cognition [7, 10, 20, 22, 24].

This manuscript has been accepted at the Human-inspired Computer Vision (HCV) ECCV 2024 Workshop as an extended abstract. A long version of the work can be found at <https://arxiv.org/abs/2408.02123v1>.

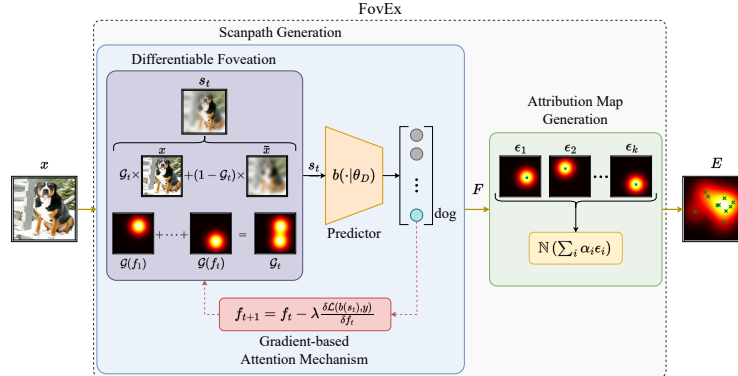


Fig. 1: FovEx. The input image x undergoes a differentiable foveation process. The loss function \mathcal{L} is exploited for the generation of a sequence of fixations (f_1, f_2, \dots, f_t) (referred to as scanpath F). F is employed to build a weighted linear combination of individual saliency maps, leading to the final attribution map E .

Contributions. We (i) introduce FovEx, a novel explanation method for deep neural networks that incorporates the biological constraint of human-foveated vision. FovEx extracts visual explanations of the predictions in a post-hoc fashion, i.e., without introducing any architectural modification to the underlying predictor. (ii) We compare FovEx to class-activation-based and perturbation-based XAI methods, achieving state-of-the-art performances for both convolutional and transformer-based models. (iii) We show that FovEx explanations can enhance human interpretability via a quantitative investigation of the correlation between human gaze patterns and the generated explanation maps.

2 Foveation-based Explanation (FovEx)

Let us consider a black-box predictor $b(\cdot|\theta)$ defined for classification problems, e.g. a neural network with learnable parameters θ . FovEx is a function $E = \text{FovEx}(b, x)$ yielding an attribution map E for the predictor b , associated to the input x , and is constituted by three fundamental operations, see Fig. 1:

(i) **Differentiable Foveation.** To model human foveated vision, we exploit a differentiable foveation mechanism [20]. Let x be an input image and f_t be the current coordinates of the focus of attention at time t . We define a coarse version of x , denoted by \bar{x} , by convolving it with a Gaussian kernel. A foveated input image x_Φ is obtained through a differentiable foveation function $\Phi(\cdot)$, defined as a weighted sum of the original input x and the coarse version of the input \bar{x} , i.e., $x_\Phi = \Phi(x, f_t) = \mathcal{W}(t) \cdot x + (1 - \mathcal{W}(t)) \cdot \bar{x}$ where $\mathcal{W}(t)$ is a weighting factor defined as a Gaussian blob with mean f_t and standard deviation σ_f .

(ii) **Gradient-based Attention Mechanism.** The foveation mechanism allows for sequential exploration of the given input image. The next location of interest (i.e., fixation point) will depend on the state s_t generated by all previous fixation locations, which can be regarded as the system’s memory. The s_t is

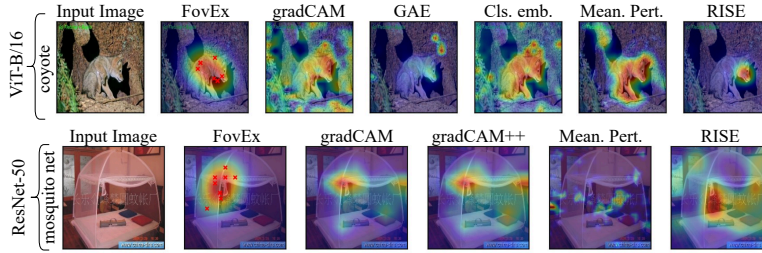


Fig. 2: Attribution maps. Explanation maps generated by FovEx and competitors for ViT-B/16 (top) and ResNet-50 (bottom).

obtained by cumulating Gaussian blobs to gradually expand the region of good visual fidelity after each fixation point, i.e., $s_t = s(x, f_t) = \mathcal{G}_t \cdot x + (\mathbb{1} - \mathcal{G}_t) \cdot \bar{x}$. The forgetting factor $0 \leq \beta \leq 1$ regulates how much information is retained from previous fixations. Let $\mathcal{L}(b(s_t), y)$ be the loss function at time t , e.g., calculated as the distance between the output predicted by b for the current state s_t and the target class y . The next fixation locations are obtained minimizing the loss function \mathcal{L} with respect to the current fixation location f_t , i.e., $f_{t+1} = f_t - \lambda \frac{\partial \mathcal{L}}{\partial f_t}$, where λ denotes the update step size. New fixations can be generated for N steps, resulting in a sequence of N fixations points, also called a *scanpath* $F = (f_1, \dots, f_N)$.

(iii) **Attribution Map Generation.** Each fixation point f_i of the scanpath can be associated with a saliency map ϵ_i , describing a 2D Gaussian with mean f_i and standard deviation σ_ϵ (σ_ϵ is set to match σ_f). The final attribution map E is obtained as a weighted linear combination of the individual saliency maps associated with each fixation point, i.e., $E = \mathbb{N} \left(\sum_{i=1}^k \alpha_i \epsilon_i \right)$, where α_i is a weighting factor for saliency map ϵ_i and $\mathbb{N}(\cdot)$ represents min-max normalization. The weights α_i determine each fixation contribution to the final saliency map.

3 Experiments

Setup & Data. We focus on FovEx’s performance for pretrained ResNet-50 [11] and a Vision Transformer (ViT-B/16) [8] on a subset of 5000 images from the ImageNet-1K [19] validation set, randomly sampled among the ones correctly classified by the predictor b , following recent literature [15]. We additionally investigate the correlation of attribution maps generated by FovEx and other competitors with the ones obtained from human gaze for image free-viewing task, exploiting the MIT1003 dataset [13]. The goal is to investigate the ability of generating explanation maps correlated to general human gaze while being faithful to a black-box model’s decision making, in order to enhance visual plausibility [14, 18]. The implementation code can be found at <https://github.com/mahadev1995/FovEx>.

Metrics. We report model performances focusing on the faithfulness (the extent to which explanation maps correspond to the behavior of the black-box model) and localization attributes of the explanation maps. We report AVG. % DROP

Table 1: ViT-B/16 (top) and ResNet-50 (bottom) quantitative evaluation. Best in bold, second best is underlined.

Eval. Name	FovEx	grad CAM	GAE	Cls. Emb.	Mean. Pert.	RISE	random CAM
AVG. % DROP (↓)	13.970	40.057	86.207	34.862	29.753	<u>15.673</u>	80.714
AVG. % INCREASE (↑)	30.389	11.469	0.799	13.329	20.549	<u>22.189</u>	1.789
DELETE (↓)	0.240	<u>0.157</u>	0.172	0.155	0.200	0.158	0.395
INSERT (↑)	0.840	<u>0.818</u>	0.806	0.817	0.674	0.782	0.682
EBPG (↑)	47.705	41.667	39.812	39.350	40.646	<u>42.633</u>	35.708

Eval. Name	FovEx	grad CAM	grad CAM++	Mean. Pert.	RISE	random CAM
AVG. % DROP (↓)	11.780	21.718	19.863	85.973	<u>11.885</u>	61.317
AVG. % INCREASE (↑)	61.849	43.669	45.069	4.700	<u>55.489</u>	16.729
DELETE (↓)	0.151	0.108	0.113	0.082	<u>0.100</u>	0.212
INSERT (↑)	0.374	0.368	0.361	0.280	<u>0.372</u>	0.287
EBPG (↑)	46.977	48.658	<u>47.412</u>	42.725	43.312	38.118

(lower is better) and AVG. % INCREASE introduced in [2] (higher is better), as well as the DELETE (lower is better), INSERT metrics (higher is better) proposed by Petsiuk *et al.* [17], and the Energy-Based Pointing Game (EBPG) localization metric [25] (higher is better). Lastly, we investigate the ability of generating explanation maps correlated to general human gaze in terms of Normalised Scan-path Similarity (NSS) and Area Under the ROC Curve Judd version (AUCJ) metrics [26].

Compared Models & Architecture Details. When considering the ViT-B/16 predictor, we report performances obtained by gradCAM [21], Meaningful Perturbation (Mean. Pert.) [9], RISE [17], GAE [3], and class embedding projection (Cls. Emb.) [23]. In the case of a ResNet-50 predictor, we consider gradCAM, gradCAM++ [2], Mean. Pert., and RISE as competitors. In all the settings, we also report a baseline technique for sanity check, referred to as RandomCAM.

Table 2: Human-gaze correlation. NSS and AUCJ metrics (higher is better).

Eval. Name	FovEx	grad CAM	grad CAM++	Cls. Emb.	GAE	Mean. Pert.	RISE
NSS (↑)	0.7160	0.2357	0.0372	0.1231	0.4120	0.6197	0.6287
AUCJ (↑)	0.7044	0.5581	0.5094	0.5317	0.6875	0.6698	0.6400

Results & Conclusions. Qualitatively, FovEx generates explanation maps that are spread over the whole object of interest without any blemish or stray spot (see Fig. 2), in contrast to the ones produced by gradCAM, GAE, and Cls. Emb., solving the issue pointed out by [6]. We report in Tab. 1 (top) the results obtained for the ViT-B/16 predictor. FovEx outperforms all the competitors across all metrics, with the exception of DELETE, where the Cls. Emb. method excels. Similar conclusions can be drawn when we consider *b* to be a ResNet-50, as reported in Tab. 1 (bottom). As shown in Tab. 2, FovEx outperforms other methods in both the considered metrics for human-gaze correlation. The achieved performances are almost doubled with respect to gradCAM and gradCAM++.

Overall, these result highlights both the superior performances w.r.t competitors and the alignment between the explanation maps produced by FovEx and human gaze patterns during free-viewing of natural images, enhancing our confidence in FovEx’s ability to close the interpretation gap between humans and machines.

References

1. Abnar, S., Zuidema, W.: Quantifying attention flow in transformers. arXiv preprint arXiv:2005.00928 (2020) [1](#)
2. Chattopadhyay, A., Sarkar, A., Howlader, P., Balasubramanian, V.N.: Grad-cam++: Generalized gradient-based visual explanations for deep convolutional networks. In: 2018 IEEE Winter Conference on Applications of Computer Vision (WACV). pp. 839–847 (2018) [1](#), [4](#)
3. Chefer, H., Gur, S., Wolf, L.: Generic attention-model explainability for interpreting bi-modal and encoder-decoder transformers. In: Proceedings of the IEEE/CVF International Conference on Computer Vision. pp. 397–406 (2021) [1](#), [4](#)
4. Chefer, H., Gur, S., Wolf, L.: Transformer interpretability beyond attention visualization. In: Proceedings of the IEEE/CVF conference on computer vision and pattern recognition. pp. 782–791 (2021) [1](#)
5. Choi, H., Jin, S., Han, K.: Adversarial normalization: I can visualize everything (ice). In: Proceedings of the IEEE/CVF Conference on Computer Vision and Pattern Recognition (CVPR). pp. 12115–12124 (June 2023) [1](#)
6. Darcet, T., Oquab, M., Mairal, J., Bojanowski, P.: Vision transformers need registers. arXiv preprint arXiv:2309.16588 (2023) [4](#)
7. Deza, A., Konkle, T.: Emergent properties of foveated perceptual systems. arXiv preprint arXiv:2006.07991 (2020) [1](#)
8. Dosovitskiy, A., Beyer, L., Kolesnikov, A., Weissenborn, D., Zhai, X., Unterthiner, T., Dehghani, M., Minderer, M., Heigold, G., Gelly, S., et al.: An image is worth 16x16 words: Transformers for image recognition at scale. arXiv preprint arXiv:2010.11929 (2020) [3](#)
9. Fong, R.C., Vedaldi, A.: Interpretable explanations of black boxes by meaningful perturbation. In: Proceedings of the IEEE international conference on computer vision. pp. 3429–3437 (2017) [4](#)
10. Han, Y., Roig, G., Geiger, G., Poggio, T.: Scale and translation-invariance for novel objects in human vision. Scientific reports **10**(1), 1411 (2020) [1](#)
11. He, K., Zhang, X., Ren, S., Sun, J.: Deep residual learning for image recognition. In: Proceedings of the IEEE conference on computer vision and pattern recognition. pp. 770–778 (2016) [3](#)
12. Hsiao, J., Chan, A.: Towards the next generation explainable ai that promotes ai-human mutual understanding. In: XAI in Action: Past, Present, and Future Applications (2023) [1](#)
13. Judd, T., Ehinger, K., Durand, F., Torralba, A.: Learning to predict where humans look. In: 2009 IEEE 12th international conference on computer vision. pp. 2106–2113. IEEE (2009) [3](#)
14. Lai, Q., Khan, S., Nie, Y., Sun, H., Shen, J., Shao, L.: Understanding more about human and machine attention in deep neural networks. IEEE Transactions on Multimedia **23**, 2086–2099 (2020) [3](#)
15. Lee, J.R., Kim, S., Park, I., Eo, T., Hwang, D.: Relevance-cam: Your model already knows where to look. In: Proceedings of the IEEE/CVF Conference on Computer Vision and Pattern Recognition. pp. 14944–14953 (2021) [3](#)

16. Morrison, K., Shin, D., Holstein, K., Perer, A.: Evaluating the impact of human explanation strategies on human-ai visual decision-making. *Proceedings of the ACM on Human-Computer Interaction* **7**(CSCW1), 1–37 (2023) [1](#)
17. Petsiuk, V., Das, A., Saenko, K.: Rise: Randomized input sampling for explanation of black-box models. In: *Proceedings of the British Machine Vision Conference (BMVC)* (2018) [4](#)
18. Qi, R., Zheng, Y., Yang, Y., Cao, C.C., Hsiao, J.H.: Explanation strategies for image classification in humans vs. current explainable ai. *arXiv preprint arXiv:2304.04448* (2023) [3](#)
19. Russakovsky, O., Deng, J., Su, H., Krause, J., Satheesh, S., Ma, S., Huang, Z., Karpathy, A., Khosla, A., Bernstein, M., Berg, A.C., Fei-Fei, L.: ImageNet Large Scale Visual Recognition Challenge. *International Journal of Computer Vision (IJCV)* **115**(3), 211–252 (2015) [3](#)
20. Schwinn, L., Precup, D., Eskofier, B., Zanca, D.: Behind the machine’s gaze: Neural networks with biologically-inspired constraints exhibit human-like visual attention. *arXiv preprint arXiv:2204.09093* (2022) [1](#), [2](#)
21. Selvaraju, R.R., Cogswell, M., Das, A., Vedantam, R., Parikh, D., Batra, D.: Grad-cam: Visual explanations from deep networks via gradient-based localization. In: *2017 IEEE International Conference on Computer Vision (ICCV)*. pp. 618–626 (2017) [1](#), [4](#)
22. Tiezzi, M., Marullo, S., Betti, A., Meloni, E., Faggi, L., Gori, M., Melacci, S.: Foveated neural computation. In: *Joint European Conference on Machine Learning and Knowledge Discovery in Databases*. pp. 19–35. Springer (2022) [1](#)
23. Vilas, M.G., Schaumlöffel, T., Roig, G.: Analyzing vision transformers for image classification in class embedding space (2023) [4](#)
24. Volokitin, A., Roig, G., Poggio, T.A.: Do deep neural networks suffer from crowding? *Advances in neural information processing systems* **30** (2017) [1](#)
25. Wang, H., Wang, Z., Du, M., Yang, F., Zhang, Z., Ding, S., Mardziel, P., Hu, X.: Score-cam: Score-weighted visual explanations for convolutional neural networks. In: *Proceedings of the IEEE/CVF conference on computer vision and pattern recognition workshops*. pp. 24–25 (2020) [4](#)
26. Zanca, D., Serchi, V., Piu, P., Rosini, F., Rufa, A.: Fixatons: A collection of human fixations datasets and metrics for scanpath similarity. *arXiv preprint arXiv:1802.02534* (2018) [4](#)